Induced Anisotropy in Rapid Flows of Nonspherical Granular Materials

Harald Ehrentraut and Agnieszka Chrzanowska

Institute of Mechanics, Darmstadt University of Technology, Hochschulstraße 1, 64289 Darmstadt, Germany, e-mail:{harald, achrzano}@mechanik.tu-darmstadt.de

received 28 Oct 2002 — accepted 11 Jan 2003

Abstract. Flow induced formation of internal order is one of the mechanisms which are responsible for changes in the effective constitutive properties of granular materials. Especially, if the grain shapes differ significantly from a sphere the possibility of flow alignment exists and it takes not much imagination to visualize that a sliding motion of the particles is affected by their mutual alignment. The approach we are taking here is based on a continuum mechanical description of a Cosserat medium with additional internal variables describing the local order of the grain orientations. An analytical description of the problem will be presented, the validity of the SAVAGE–HUTTER theory for anisotropic granular media will be discussed, and experimental findings are compared to the theoretical results.

1 Granular Dynamics

Granular materials are special for many reasons: First of all, they appear in many parts of nature and they play an important role in many technical applications. Secondly, granular materials behave quite differently at rest and under flow conditions; where elastoplastic effects dominate the material response of undisturbed samples, even small perturbations can switch their solid-like response to fluid-like material behavior. Thirdly, granular materials are neither really macroscopic nor microscopic systems – although the overall material properties depend on the interaction of a huge number of particles (thus resembling systems subjected to the methods of statistical mechanics like molecular gases or fluids) the particles themselves are macroscopic objects. Consequently, the interaction of these constituents is dissipative which distinguishes granular media from typical molecular systems.

This hybrid behavior of granular media shows up also in the methods used to model their constitutive properties. Dissipative molecular dynamics is certainly a good way to gain some insight about these materials. However, if the number of model particles is strongly increased, if a three-dimensional model is needed or if the particle shapes are rather irregular the necessary computational power easily exceeds all available resources. Thus, computer simulations based on particle dynamics are very useful to test special cases but they do not provide a universal method to solve engineering problems. On the other hand, a continuum mechanical approach can be used. As it is the case in all continuum theories the amount of microscopical information is so much reduced that the mean behavior of the constituents can be described, but all effects concerning only a small number of

K. Hutter et al. (eds.), *Dynamic Response of Granular and Porous Materials under Large and Catastrophic Deformations*

particles are not covered by this approach. Normally, this does not pose a problem for typical materials (solids, liquids, or gases); continuum theories are being used, since the constituents are of microscopic size and typical length scales of particle dimensions and macroscopically relevant distances differ by many orders of magnitude. In granular dynamics, however, the difference between both length scales is often much less. In a rock avalanche, e.g., the trajectory of a single boulder might be very important. The deposition of scattered debris at the outrun of an avalanche is also not covered by continuum methods and the spontaneous blocking of granular flows in a constriction (like at the outlet of a silo) is initially being caused by wedging of just a few particles. Thus, there is no universal theory in sight which can cover all aspects of granular behavior but one has to decide which phenomenons should be modeled and which method is suited best for this purpose.

The approach taken in the present paper belongs clearly to the continuum theoretical side. Thus, there are no "particles" entering the description and no microscopic evolution equations are being used. If we speak, however, occasionally of particles it is just to refer to an underlying microscopic description and to motivate ideas about physical properties which influence either the dynamical equations (balances) or the constitutive relations. Details about the transition from a purely microscopic theory to a continuum description through some averaging procedure ("coarse graining" or "time smoothing") can be found in many places in the literature.

1.1 Balance Equations and Constitutive Relations

Let us start from a very basic assumption about the grains of a granular medium: We assume that they are nearly rigid, the grain–grain as well as the grain–wall (or grain–bottom) contact involves friction, and each grain is capable of a gliding and spinning motion (resulting in six degrees of freedom for each grain). The grains may have any shape (although we shall consider mostly special, simple cases), but the size of the grains is assumed to be fairly constant – otherwise we have to resort to a mixture theory which is, of course, possible but complicates the description further and is out of scope for this treatise. We do not consider a matrix fluid filling the gaps between the grains, i.e. we are dealing with dry granular materials.

Since a volume element for the continuum mechanical description must contain a large number of particles and an ensemble of rigid bodies *does not* behave again rigidly, we have to write down the balance equations of a mesomorphic Cosserat medium: the constituents of the medium are deformable, couple stresses exist for the internal interaction and the angular momentum contains not only moment of momentum but also spin. If we denote the mass density by ρ, the velocity field by $\boldsymbol{v}$, the Cauchy stress tensor by $\underline{\underline{\mathrm{t}}}$, the specific external force density by $\boldsymbol{f}$, the specific spin density by $\boldsymbol{s}$, the couple stresses by $\underline{\underline{\pi}}$ and the external specific torque density by $\boldsymbol{m}$, the balance equations are as follows (the symbol $^\top$ denotes transposition):

$$\frac{\partial}{\partial t}\rho + \nabla\cdot(\rho\boldsymbol{v}) = 0\,, \tag{1a}$$

$$\frac{\partial}{\partial t}(\rho\boldsymbol{v}) + \nabla\cdot\Big(\rho\boldsymbol{v}\boldsymbol{v} - \underline{\underline{\mathrm{t}}}^\top\Big) = \rho\boldsymbol{f}\,, \tag{2a}$$

$$\frac{\partial}{\partial t}\Big(\rho(\boldsymbol{x}\times\boldsymbol{v}+\boldsymbol{s})\Big) + \nabla\cdot\Big(\rho\boldsymbol{v}(\boldsymbol{x}\times\boldsymbol{v}+\boldsymbol{s}) - (\boldsymbol{x}\times\underline{\underline{\mathrm{t}}})^\top - \underline{\underline{\pi}}^\top\Big) = \rho\Big(\boldsymbol{x}\times\boldsymbol{f}+\boldsymbol{m}\Big)\,. \tag{3a}$$

Equation (1a) constitutes (of course) conservation of mass, (2a) is the momentum balance, and the balance of angular momentum (3a) does not reduce to a symmetry requirement of the stress tensor. To go further, we assume incompressible, gravity-driven flows – ρ is a constant ρ_0, $\boldsymbol{f}$ is the gravitational acceleration $\boldsymbol{g}$ and no external torques are present, i.e. $\boldsymbol{m} = \boldsymbol{0}$ – and we remove the contributions due to the balances of mass and momentum in the balance of angular momentum. The new set of balances reads now

$$\nabla\cdot\boldsymbol{v} = 0\,, \tag{1b}$$

$$\rho_0\Big(\frac{\partial}{\partial t}\boldsymbol{v} + \nabla\cdot(\boldsymbol{v}\boldsymbol{v})\Big) = \nabla\cdot\underline{\underline{\mathrm{t}}}^\top + \rho_0\boldsymbol{g}\,, \tag{2b}$$

$$\rho_0\,\frac{d}{dt}\boldsymbol{s} = \boldsymbol{\epsilon}:\underline{\underline{\mathrm{t}}} + \nabla\cdot\boldsymbol{\pi}^\top\,. \tag{3b}$$

Here, $\boldsymbol{\epsilon}$ denotes the LEVI-CIVITA tensor and

$$\frac{d}{dt} = \frac{\partial}{\partial t} + \boldsymbol{v}\cdot\nabla$$

is the material time derivative. In addition, the balance of energy is needed. If one eliminates all contributions due to conservation of mass, momentum and angular momentum from the balance of energy, one obtains the balance equation for the internal energy e

$$\rho\frac{d}{dt}e + \nabla\cdot\boldsymbol{q} - \underline{\underline{\mathrm{t}}}:\nabla\boldsymbol{v} - \underline{\underline{\pi}}:\nabla\boldsymbol{\omega} + \boldsymbol{\omega}\cdot\boldsymbol{\epsilon}:\underline{\underline{\mathrm{t}}} = \rho r\,. \tag{4a}$$

Here, $\boldsymbol{q}$ denotes the heat flux (conductive transport of energy), $\boldsymbol{\omega}$ is the angular velocity – related by $\boldsymbol{s} = \underline{\underline{\Theta}}\cdot\boldsymbol{\omega}$ ($\underline{\underline{\Theta}}$: tensor of inertia) to the spin field $\boldsymbol{s}$ – and r is the supply of energy. For the granular media we want to discuss, the energy supply vanishes – $r = 0$ – and if we do not consider vibrating walls or a vibrating bed the conductive exchange of energy between medium and environment is also negligible, i.e. $\boldsymbol{q} = \boldsymbol{0}$. Then, the balance of internal energy is simply determined by the powers of stresses and couple stresses

$$\rho\frac{d}{dt}e = \underline{\underline{\mathrm{t}}}:\nabla\boldsymbol{v} + \underline{\underline{\pi}}:\nabla\boldsymbol{\omega} - \boldsymbol{\omega}\cdot\boldsymbol{\epsilon}:\underline{\underline{\mathrm{t}}}\,. \tag{4b}$$

Before we continue, a short discussion of the relevant terms in the balances is in order. Tangential friction between particles plays an important role for the stability of a granular material and also, of course, for the torque distribution inside the medium. However, if the granular medium is rapidly moving the main interaction between its constituents is due to collisions where the momentum transfer (for a-spherical particles!) is also connected with an exchange of spin. Thus, tangential friction is of less importance for granular flows and we shall disregard its contributions in the following, meaning that we set the couple stress tensor $\underline{\underline{\pi}}$ to zero,

$$\underline{\underline{\pi}} \approx \underline{\underline{\mathbf{0}}} . \tag{5}$$

Nevertheless, one should be aware of the limits of this approximation: For very small flow velocities and in situations where blocking and formation of arcs inside the material becomes a possibility, we can no longer exclude the couple stresses from our equations. If we decompose the stress tensor $\underline{\underline{\mathbf{t}}}$ into its isotropic part $-p\underline{\underline{\mathbf{1}}}$, the symmetric traceless part $\overline{\underline{\underline{\mathbf{t}}}}$ and a skew-symmetric part $\underline{\underline{\mathbf{t}}}^a$,

$$\underline{\underline{\mathbf{t}}} = -p\underline{\underline{\mathbf{1}}} + \overline{\underline{\underline{\mathbf{t}}}} + \underline{\underline{\mathbf{t}}}^a , \tag{6}$$

then the term $\underline{\underline{\mathbf{t}}} : \nabla \boldsymbol{v}$ reduces to

$$\begin{aligned} \underline{\underline{\mathbf{t}}} : \nabla \boldsymbol{v} &= -p\underbrace{\nabla \cdot \boldsymbol{v}}_{=0} + \overline{\underline{\underline{\mathbf{t}}}} : \overline{\nabla \boldsymbol{v}} + \underline{\underline{\mathbf{t}}}^a : (\nabla \boldsymbol{v})^a \\ &= \underline{\underline{\mathbf{t}}} : \underline{\underline{\mathbf{D}}} + \underline{\underline{\mathbf{t}}} : \underline{\underline{\mathbf{W}}} , \end{aligned} \tag{7}$$

where $\underline{\underline{\mathbf{D}}} := \overline{\nabla \boldsymbol{v}}$ is the stretching or shear rate tensor and $\underline{\underline{\mathbf{W}}} := (\nabla \boldsymbol{v})^a$ is the spin or vorticity tensor. Finally, we can express $\underline{\underline{\mathbf{W}}}$ easily by the vorticity vector $\boldsymbol{\Omega} := 1/2\, \nabla \times \boldsymbol{v}$

$$\underline{\underline{\mathbf{W}}} = \boldsymbol{\epsilon} \cdot \boldsymbol{\Omega} , \tag{8}$$

and arrive at the set of simplified balance equations for granular flows

$$\nabla \cdot \boldsymbol{v} = 0 , \tag{9a}$$

$$\rho_0 \Big(\frac{\partial}{\partial t} \boldsymbol{v} + \nabla \cdot (\boldsymbol{v}\boldsymbol{v}) \Big) = \nabla \cdot \underline{\underline{\mathbf{t}}}^{\top} + \rho_0 \boldsymbol{g} , \tag{9b}$$

$$\rho_0 \frac{d}{dt} \boldsymbol{s} = \boldsymbol{\epsilon} : \underline{\underline{\mathbf{t}}} , \tag{9c}$$

$$\rho_0 \frac{d}{dt} e = \underline{\underline{\mathbf{t}}} : \underline{\underline{\mathbf{D}}} + (\boldsymbol{\Omega} - \boldsymbol{\omega}) \cdot \boldsymbol{\epsilon} : \underline{\underline{\mathbf{t}}} . \tag{9d}$$

For spherical particles the stresses *are* symmetric and consequently the spin $\boldsymbol{s}$ is a constant of motion. Furthermore, we obtain $\boldsymbol{s} = \mathbf{0}$ in that case since this holds certainly true for the material at rest and conservation of spin implies the vanishing of $\boldsymbol{s}$ always. This, of course, is a direct consequence of our disregard of tangential friction – the particles are sliding, but rolling does not occur.

In addition to the differential equations (9a) – (9d) boundary conditions are needed. Here, we have to distinguish between free boundaries and boundaries where the granular medium is in contact with a wall or the bottom. Let $F^S(\boldsymbol{x}, t) := z - z^S(x, y, t) = 0$ be the implicit definition of the free surface and $F^B(\boldsymbol{x}, t) := z^B(x, y, t) - z = 0$ likewise define the contact between granular material and the bottom (if walls are present, additional functions have to be considered). z^S and

z^B are the z-coordinates of free and bottom surface, respectively, measured in normal direction from the reference surface point (x, y). All surfaces are subjected to kinematic boundary conditions ($\boldsymbol{v}^S$ and $\boldsymbol{v}^B$ are the mapping velocities of the free and basal surfaces, respectively):

$$\frac{\partial F^S}{\partial t} + \boldsymbol{v}^S \cdot \nabla F^S = 0\,, \tag{10}$$

$$\frac{\partial F^B}{\partial t} + \boldsymbol{v}^B \cdot \nabla F^B = 0\,. \tag{11}$$

In many applications, the basal topography will be independent of time, $F^B(\boldsymbol{x}) = 0$, and (11) reduces to the geometric condition $\boldsymbol{v}^B \cdot \nabla F^B = 0$ that bottom velocities are tangential to the basal surface – there is neither in- nor outflux at the base. However, kinematic boundary conditions are not enough to produce a well-posed problem. Here, they have to be supplemented by traction boundary conditions which brings us to the problem of constitutive relations for granular materials. If we would have considered couple stresses, too, torque boundary conditions would also have been necessary.

The most simple (and probably most successful) material law for granular media is of the MOHR-COULOMB type. Following again SAVAGE and HUTTER [21], dry friction with a simple proportionality between normal pressure and shear stress S for the sliding material is assumed. In addition, a yield stress $N \tan\phi$ with a material constant ϕ, called the internal friction angle, shall describe the plastic deformation of the yielding material. Thus, the relation between S and N for the yielding material is simply

$$|S| = N \tan\phi\,. \tag{12}$$

To formulate traction boundary conditions we assume a traction free upper surface (the very small friction between air and the granular material is being neglected) and a COULOMB law for friction between the sliding material and the fixed base,

$$\underline{\underline{\mathbf{t}}}^S \cdot \boldsymbol{n}^S = \mathbf{0}\,, \tag{13}$$

$$-N^B \boldsymbol{n}^B - \underline{\underline{\mathbf{t}}}^B \cdot \boldsymbol{n}^B = \hat{\boldsymbol{v}}^B N^B \tan\delta\,, \tag{14}$$

is being assumed (a hat ˆ denotes a unit vector, e.g. $\hat{\boldsymbol{v}} := \boldsymbol{v}/\|\boldsymbol{v}\|$). The normal pressure $N^B = -\boldsymbol{n}^B \cdot \underline{\underline{\mathbf{t}}}^B \cdot \boldsymbol{n}^B$ at the bottom is related to the stress by an additional material constant δ, the basal angle of friction. By $\boldsymbol{n}^B$ and $\boldsymbol{n}^S$ we denote the (outward pointing) normal vectors at the base and at the upper free surface, respectively.

1.2 Savage–Hutter Equations for Anisotropic Media

If we want to describe the granular motion along an incline or, more complicated, the evolution of an avalanche following the complex topography of a mountain slope, we have to reformulate the balances (9a) – (9d) for topography-adapted coordinates and apply a proper scaling to simplify the resulting equations. Both has been done first by SAVAGE & HUTTER [21] for the one-dimensional case and has been extended by GRAY, GREVE, HUTTER, KOCH and WIELAND up to the full, three-dimensional equations [10,11]. Let us briefly recall the procedure and see where anisotropic effects may enter the equations.

To begin, we introduce curvilinear coordinates and the appropriate local GAUSSIAN basis to parameterize the bottom topography. Let $\{\boldsymbol{i}, \boldsymbol{j}, \boldsymbol{k}\}$ denote the canonical CARTESIAN basis of three-dimensional space and let

$$\boldsymbol{c}(x) = a(x)\boldsymbol{i} + b(x)\boldsymbol{k}, \quad (x \in [0, L]) \tag{15}$$

be a parameterized curve in the $\boldsymbol{i}, \boldsymbol{k}$-plane where x denotes the arc-length, a and b are the (differentiable) component functions and L is the total length of the curve. Then we can define a reference surface by parallel translation of the curve in the $\boldsymbol{j}$-direction and measure the topography by its elevation in normal direction with respect to the reference surface (compare Fig. 1). Since we denoted the arc-length of

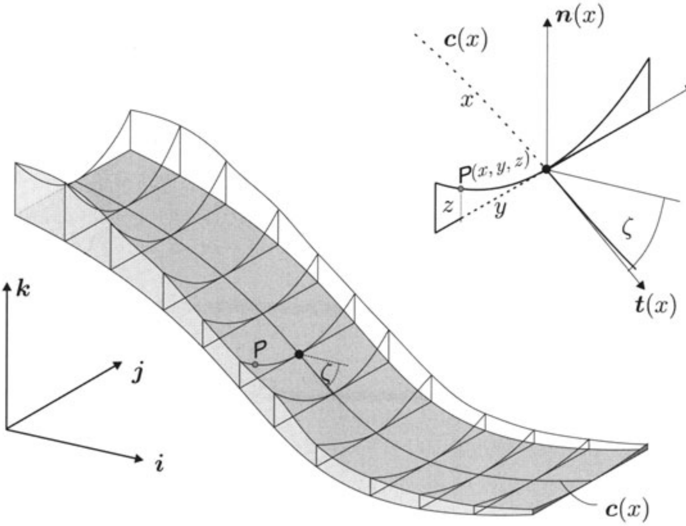

Fig. 1. Definition of the SAVAGE–HUTTER coordinates for a complex bed topography

$\boldsymbol{c}(x)$ by x, it is natural to denote the coordinate in $\boldsymbol{j}$-direction by y (x and y yield a parameterization of the reference surface) and the elevation in normal direction by z. In addition to the CARTESIAN basis we have the local GAUSSIAN basis $\{\boldsymbol{b}_x, \boldsymbol{b}_y, \boldsymbol{b}_z\}$ defined by

$$\boldsymbol{b}_q := \frac{\partial \boldsymbol{x}(x, y, z)}{\partial q} \qquad \text{for } q = x, y, z\,. \tag{16}$$

It is advantageous to use also the basal inclination angle $\zeta(x)$ of the curve $\boldsymbol{c}$ with respect to the horizontal $\boldsymbol{i}$-direction – with the convention $\zeta < 0$ for downhill and $\zeta \geq 0$ for horizontal and uphill directions. If we denote the unit tangential vector $\boldsymbol{c}'(x)$ by $\boldsymbol{t}(x)$ and the upper normal vector orthogonal to the reference plain by

$\boldsymbol{n}(x)$, we obtain finally

$$\boldsymbol{b}_x = \left(1 - z\zeta'\right)\boldsymbol{t}(x)\,, \quad \boldsymbol{b}_y = \boldsymbol{j}\,, \quad \boldsymbol{b}_z = \boldsymbol{n}(x)\,, \tag{17}$$

$$\boldsymbol{b}^x = \frac{1}{1 - z\zeta'}\,\boldsymbol{t}(x)\,, \quad \boldsymbol{b}^y = \boldsymbol{j}\,, \quad \boldsymbol{b}^z = \boldsymbol{n}(x)\,, \tag{18}$$

$$((g_{ij})) = \mathrm{diag}\left(1 - z\zeta', 1, 1\right) \ (\text{ i.e. } ds^2 = (1 - z\zeta')^2 dx^2 + dy^2 + dz^2\ )\,, \tag{19}$$

for the basis $\{\boldsymbol{b}_q\}$, the dual basis $\{\boldsymbol{b}^q\}$ and the matrix $((g_{ij}))$ of metric coefficients. The local bases are therefore orthogonal but not normalized. The co-variant derivative ∇ along the surface, expressed in the natural basis and coordinates, is consequently

$$\nabla = \boldsymbol{b}^x \frac{\partial}{\partial x} + \boldsymbol{b}^y \frac{\partial}{\partial y} + \boldsymbol{b}^z \frac{\partial}{\partial z}\,. \tag{20}$$

To abbreviate and to be consistent with literature we use $\Psi := (1 - z\zeta)^{-1}$ and $\kappa := \zeta'$ (κ is the curvature of $\boldsymbol{c}$). For any differentiable vector field $\boldsymbol{v} = u\boldsymbol{t} + v\boldsymbol{j} + w\boldsymbol{n}$, expressed in the local, *normalized* basis by its (x, y, z)-dependent component functions u, v, w, we arrive at the formula

$$\begin{aligned} \nabla \cdot \boldsymbol{v} &= \Psi\frac{\partial u}{\partial x} + \frac{\partial v}{\partial y} + \frac{\partial w}{\partial z} - \Psi\kappa w \\ &= \frac{\partial(\Psi u)}{\partial x} + \frac{\partial v}{\partial y} + \frac{\partial w}{\partial z} - \Psi\kappa w - \Psi^2\kappa' uz \end{aligned} \tag{21}$$

for the divergence of a vector field, and

$$\begin{aligned} \nabla \cdot \underline{\underline{\mathrm{T}}} = &\Big(\frac{\partial}{\partial x}(\Psi T_{xx}) + \frac{\partial}{\partial y}T_{yx} + \frac{\partial}{\partial z}T_{zx} - \Psi\kappa(T_{xz} + T_{zx}) - \Psi^2\kappa' z T_{xx}\Big)\boldsymbol{t} \\ &+ \Big(\frac{\partial}{\partial x}(\Psi T_{xy}) + \frac{\partial}{\partial y}T_{yy} + \frac{\partial}{\partial z}T_{zy} - \Psi\kappa T_{zy} - \Psi^2\kappa' z T_{xy}\Big)\boldsymbol{j} \\ &+ \Big(\frac{\partial}{\partial x}(\Psi T_{xz}) + \frac{\partial}{\partial y}T_{yz} + \frac{\partial}{\partial z}T_{zz} - \Psi\kappa(T_{zz} - T_{xx}) - \Psi^2\kappa' z T_{xz}\Big)\boldsymbol{n} \end{aligned} \tag{22}$$

for the divergence of a tensor field $\underline{\underline{\mathrm{T}}}$ of second order. Please note that no symmetry of $\underline{\underline{\mathrm{T}}}$ was assumed and therefore the formula in (22) differs slightly from the expression used in the extended SAVAGE–HUTTER theory by GRAY, WIELAND & HUTTER [10].

Now we can rewrite (9a) and (9b) using curvilinear coordinates. We obtain for the balance of mass (u, v, w shall denote the velocity components)

$$\frac{\partial}{\partial x}(\Psi u) + \frac{\partial v}{\partial y} + \frac{\partial w}{\partial z} - \Psi\kappa w - \Psi^2\kappa' zu = 0\,. \tag{23}$$

From the balance of momentum (9b) we derive the set of equations

$$\rho_0\Big\{\frac{\partial u}{\partial t}+\frac{\partial}{\partial x}(\Psi u^2)+\frac{\partial}{\partial y}(uv)+\frac{\partial}{\partial z}(uw)-2\Psi\kappa uw-\Psi^2\kappa' zu^2\Big\}$$
$$=-\rho_0 g\sin\zeta+\frac{\partial}{\partial x}(\Psi t_{xx})+\frac{\partial}{\partial y}t_{xy}+\frac{\partial}{\partial z}t_{xz}-\Psi\kappa(t_{zx}+t_{xz})-\Psi^2\kappa' zt_{xx}\,, \tag{24}$$

$$\rho_0\Big\{\frac{\partial v}{\partial t}+\frac{\partial}{\partial x}(\Psi uv)+\frac{\partial}{\partial y}v^2+\frac{\partial}{\partial z}(vw)-\Psi\kappa vw-\Psi^2\kappa' zuv\Big\}$$
$$=\frac{\partial}{\partial x}(\Psi t_{yx})+\frac{\partial}{\partial y}t_{yy}+\frac{\partial}{\partial z}t_{yz}-\Psi\kappa t_{yz}-\Psi^2\kappa' zt_{yx}\,, \tag{25}$$

$$\rho_0\Big\{\frac{\partial w}{\partial t}+\frac{\partial}{\partial x}(\Psi uw)+\frac{\partial}{\partial y}(vw)+\frac{\partial}{\partial z}w^2-\Psi\kappa(w^2-u^2)-\Psi^2\kappa' zuw\Big\}$$
$$=-\rho_0 g\cos\zeta+\frac{\partial}{\partial x}(\Psi t_{zx})+\frac{\partial}{\partial y}t_{zy}+\frac{\partial}{\partial z}t_{zz}-\Psi\kappa(t_{zz}-t_{xx})-\Psi^2\kappa' zt_{zx}\,. \tag{26}$$

We denote the components of the specific spin density $\boldsymbol{s}=\alpha\boldsymbol{t}+\beta\boldsymbol{j}+\gamma\boldsymbol{n}$ by α, β and γ. Then the spin balance (9c) results in

$$\rho_0\Big\{\frac{\partial\alpha}{\partial t}+\Psi u\frac{\partial\alpha}{\partial x}+v\frac{\partial\alpha}{\partial y}+w\frac{\partial\alpha}{\partial z}-\Psi\kappa u\gamma\Big\}=t_{yz}-t_{zy}\,, \tag{27}$$

$$\rho_0\Big\{\frac{\partial\beta}{\partial t}+\Psi u\frac{\partial\beta}{\partial x}+v\frac{\partial\beta}{\partial y}+w\frac{\partial\beta}{\partial z}\Big\}=t_{zx}-t_{xz}\,, \tag{28}$$

$$\rho_0\Big\{\frac{\partial\gamma}{\partial t}+\Psi u\frac{\partial\gamma}{\partial x}+v\frac{\partial\gamma}{\partial y}+w\frac{\partial\gamma}{\partial z}+\Psi\kappa u\alpha\Big\}=t_{xy}-t_{yx}\,. \tag{29}$$

The balance equations (9a) – (9c) provide information about the mechanical behavior of a granular flow. The balance of internal energy (9d), however, becomes important whenever the dissipated energy during the sliding motion of the material becomes so large that a noticeable increase of internal energy (or temperature, the conjugated thermodynamic variable) occurs. Thus, the importance of (9d) depends on the flow situation: Under "normal" conditions the heat generated by bed and internal friction is quite small and we can disregard the energy equation and concentrate on the mechanical equations alone. On the other hand, an increase of temperature may modify friction angles and other constitutive variables. If the dissipation in the flow is therefore high (as, e.g., in alpine rock slides), the energy equation becomes important and we have to treat the full system of equations.

For our purposes here, we shall assume granular flows with small dissipation and consider (9d) only in connection with the second law of thermodynamics, but *not* as a necessary equation for solving the problem of motion.

The thickness of flow avalanches is usually much smaller than their lateral extensions, i.e. an avalanche is a shallow object and we can reduce the dimensionality of the flow problem by depth integration. Indeed, this was done by SAVAGE & HUTTER after scaling the balances of mass and momentum. Following the approach by GRAY, HUTTER, WIELAND and TAI [22] we postpone any scaling and integrate the equations (9a) – (9c) directly over the thickness $h=z^S-z^B$ of the granular body. This average will be denoted by a bar,

$$\bar{g}(x,y,t):=\frac{1}{h(x,y,t)}\int\limits_{z^B(x,y,t)}^{z^S(x,y,t)} g(x,y,z,t)\,dz\,. \tag{30}$$

Since the derivatives with respect to z turn into surface terms of the free and bottom surface, the boundary conditions (10) – (14) must be rewritten, too, and we obtain

$$-\frac{\partial z^S}{\partial t} - \Psi^S u^S \frac{\partial z^S}{\partial x} - v^S \frac{\partial z^S}{\partial y} + w^S = 0\,, \tag{31}$$

$$\frac{\partial z^B}{\partial t} + \Psi^B u^B \frac{\partial z^B}{\partial x} + v^B \frac{\partial z^B}{\partial y} - w^B = 0\,, \tag{32}$$

for the kinematic boundary conditions,

$$t_{xx}^S \Psi^S \frac{\partial z^S}{\partial x} + t_{xy}^S \frac{\partial z^S}{\partial y} - t_{xz}^S = 0\,, \tag{33}$$

$$t_{yx}^S \Psi^S \frac{\partial z^S}{\partial x} + t_{yy}^S \frac{\partial z^S}{\partial y} - t_{yz}^S = 0\,, \tag{34}$$

$$t_{zx}^S \Psi^S \frac{\partial z^S}{\partial x} + t_{zy}^S \frac{\partial z^S}{\partial y} - t_{zz}^S = 0\,, \tag{35}$$

for the stress-free surface and

$$-t_{xx}^B \Psi^B \frac{\partial z^B}{\partial x} - t_{xy}^B \frac{\partial z^B}{\partial y} + t_{xz}^B = \left(\|\nabla F^B\| \hat{u}^B \tan\delta + \Psi^B \frac{\partial z^B}{\partial x} \right) N^B\,, \tag{36}$$

$$-t_{yx}^B \Psi^B \frac{\partial z^B}{\partial x} - t_{yy}^B \frac{\partial z^B}{\partial y} + t_{yz}^B = \left(\|\nabla F^B\| \hat{v}^B \tan\delta + \Psi^B \frac{\partial z^B}{\partial y} \right) N^B\,, \tag{37}$$

$$-t_{zx}^B \Psi^B \frac{\partial z^B}{\partial x} - t_{zy}^B \frac{\partial z^B}{\partial y} + t_{zz}^B = \left(\|\nabla F^B\| \hat{w}^B \tan\delta - 1 \right) N^B \tag{38}$$

for the sliding boundary condition at the base.

The depth integrated balance of mass has, of course, been already obtained by GRAY, WIELAND & HUTTER and reads [10]

$$\frac{\partial h}{\partial t} + \frac{\partial}{\partial x}(h\overline{\Psi u}) + \frac{\partial}{\partial y}(h\bar{v}) - \kappa' h \overline{\Psi^2 z u} - 2\kappa h \overline{\Psi w} = 0\,. \tag{39}$$

Integration of the balances of momentum yields

$$\rho_0\Big\{\frac{\partial}{\partial t}(h\bar{u})+\frac{\partial}{\partial x}(h\overline{\Psi u^2})+\frac{\partial}{\partial y}(h\overline{uv})-2h\kappa\overline{\Psi uw}-h\kappa'\overline{\Psi^2 zu^2}\Big\}$$
$$=-\rho_0 hg\sin\zeta+\frac{\partial}{\partial x}(h\overline{\Psi t_{xx}})+\frac{\partial}{\partial y}(h\overline{t_{xy}})-h\kappa\overline{\Psi(t_{zx}+t_{xz})}$$
$$-h\kappa'\overline{\Psi^2 zt_{xx}}+N^B(\Psi^B\frac{\partial z^B}{\partial x}+\|\nabla F^B\|\hat{u}^B\tan\delta)\,, \tag{40}$$

$$\rho_0\Big\{\frac{\partial}{\partial t}(h\bar{v})+\frac{\partial}{\partial x}(h\overline{\Psi vu})+\frac{\partial}{\partial y}(h\overline{v^2})-h\kappa\overline{\Psi vw}-h\kappa'\overline{\Psi^2 zuv}\Big\}$$
$$=\frac{\partial}{\partial x}(h\overline{\Psi t_{yx}})+\frac{\partial}{\partial y}(h\overline{t_{yy}})-h\kappa\overline{\Psi t_{zy}}$$
$$-h\kappa'\overline{\Psi^2 zt_{xy}}+N^B(\Psi^B\frac{\partial z^B}{\partial x}+\|\nabla F^B\|\hat{v}^B\tan\delta)\,, \tag{41}$$

$$\rho_0\Big\{\frac{\partial}{\partial t}(h\bar{w})+\frac{\partial}{\partial x}(h\overline{\Psi uw})+\frac{\partial}{\partial y}(h\overline{wv})-h\kappa\overline{\Psi(w^2-u^2)}-h\kappa'\overline{\Psi^2 zuw}\Big\}$$
$$=-\rho_0 hg\cos\zeta+\frac{\partial}{\partial x}(h\overline{\Psi t_{zx}})+\frac{\partial}{\partial y}(h\overline{t_{zy}})-h\kappa\overline{\Psi(t_{zz}-t_{xx})}$$
$$-h\kappa'\overline{\Psi^2 zt_{zx}}+N^B(1-\|\nabla F^B\|\hat{w}^B\tan\delta)\,. \tag{42}$$

The only difference to the equations obtained by GRAY, WIELAND & HUTTER is again the symmetry of the stresses which we do not presuppose at this time. Thus, we have additional three equations from the spin balance ($\boldsymbol{s}=\alpha\boldsymbol{t}+\beta\boldsymbol{j}+\gamma\boldsymbol{n}$)

$$\rho_0\Big\{\frac{\partial}{\partial t}(h\bar{\alpha})+\frac{\partial}{\partial x}(h\overline{\Psi u\alpha})+\frac{\partial}{\partial y}(h\overline{v\alpha})-\kappa(\overline{\Psi\alpha w}+\overline{\Psi\gamma u})\Big\}=\overline{t_{yz}}-\overline{t_{zy}}\,, \tag{43}$$

$$\rho_0\Big\{\frac{\partial}{\partial t}(h\bar{\beta})+\frac{\partial}{\partial x}(h\overline{\Psi u\beta})+\frac{\partial}{\partial y}(h\overline{v\beta})-\kappa\overline{\Psi\beta w}\Big\}=\overline{t_{zx}}-\overline{t_{xz}}\,, \tag{44}$$

$$\rho_0\Big\{\frac{\partial}{\partial t}(h\bar{\gamma})+\frac{\partial}{\partial x}(h\overline{\Psi u\gamma})+\frac{\partial}{\partial y}(h\overline{v\gamma})-\kappa(\overline{\Psi\gamma w}-\overline{\Psi\alpha u})\Big\}=\overline{t_{xy}}-\overline{t_{yx}}\,, \tag{45}$$

which supplement the "normal" set of equations of the SAVAGE–HUTTER theory.

The next step in the derivation of the final set of equations is the scaling which determines the physically relevant terms. We assume:

- The aspect ratio $\epsilon=H/L$ (H being the maximum thickness of the avalanche and L denoting the typical length of the flowing body) of the granular avalanche is in most flow situations rather small (i.e. $\epsilon\ll 1$),
- the curvature $\kappa=\tilde{\kappa}/R$ with R/L is at most of order ϵ,
- the shear/normal stress ratios t_{ij}/t_{kk} ($i\neq j$ and i,j,k taking values in (x,y,z)) are of order ϵ [11], and
- typical "vertical" velocities w are also of ϵ-order of magnitude.

Then the SAVAGE–HUTTER equations are obtained from the balances of mass and momentum. The interested reader can find a detailed presentation in [10] which we shall not repeat here.

The agreement between experiment and the predictions of the SAVAGE–HUTTER theory as reported in [10] is very convincing, and the question might be asked if it is really necessary to amend the set of equations in the case of non-spherical grains or if the *same* set of equations is capable to describe anisotropic flows.

Indeed, the crucial terms here are the shear stress differences $t_{ij} - t_{ji}$ which act as torque density in the spin balance. One of the assumptions of the SAVAGE–HUTTER theory is that all shear stresses are of the same order of magnitude. In this approximation, their difference would be much smaller than a typical shear stress and the asymmetry of the stress tensor turns out to be (at least) a second order effect. However, we can tackle the problem of the spin balance also from a dynamical point of view. Since granular flows are rather dense, each grain is confined in a narrow region of space bounded by its nearest neighbors which form some kind of cage. Especially when the grain shape differs significantly from a sphere the rotational mobility of single grains is therefore strongly hindered and it is reasonable to assume that typical values of the spin $h\alpha$ (or any other spin component) are at least as small as the vertical velocity w, i.e. we would have to assume a scaling law

$$h(\alpha,\beta,\gamma) = (gL)^{1/2}\epsilon^{\sigma}(\tilde{\alpha},\tilde{\beta},\tilde{\gamma}) \quad \text{with } \sigma \geq 1. \tag{46}$$

Then the equations (43) – (45) tell us that the shear stress differences are of the same orders, too, and the asymmetry of the stress tensor in the momentum balance is a correction term of higher order than those contributing to the SAVAGE–HUTTER equations.

Thus we can conclude: The SAVAGE–HUTTER equations in the form of [10] provide an adequate description even for anisotropic granular materials. For a granular system without any tangential friction of the grains the asymmetry of the stress tensor becomes only important when higher order effects are investigated. The additional equations for anisotropic granular media in the limit of the SAVAGE–HUTTER theory reduce consequently to a symmetry statement:

$$\overline{t_{yz}} - \overline{t_{zy}} = 0\,, \tag{47}$$
$$\overline{t_{zx}} - \overline{t_{xz}} = 0\,, \tag{48}$$
$$\overline{t_{xy}} - \overline{t_{yx}} = 0 \tag{49}$$

However, we can *not* start from symmetric a priori expressions for the stresses. The symmetry conditions (47) – (49) provide additional information which determine the internal structure of the granular medium.

This fact becomes of particular importance when we consider processes which are capable of orienting the particles in the granular material. Such processes have to break the isotropic symmetry of space which, however, occurs in many situations. Probably the most important mechanisms of symmetry breaking for granular materials occurs in shear bands. Flow and gradient direction in a simple shear distinguish certain spatial directions and the vorticity of the flow field yields an effective torque acting on the particles in the flow. Therefore, we expect some influence of the shear on the internal structure of the granular material. The exploitation of the symmetry conditions (47) – (49) to derive an analytical description of the shear induced anisotropy is subject of the next section.

2 Constitutive Relations and Order Parameters

In an anisotropic granular material, which is slowly flowing down a flat incline, nothing spectacular happens: A stationary plug flow develops, the grains are randomly oriented (see Fig. 2) and virtually no shear layer occurs at the bottom if the basal friction is not too high. The situation changes when we increase the mean

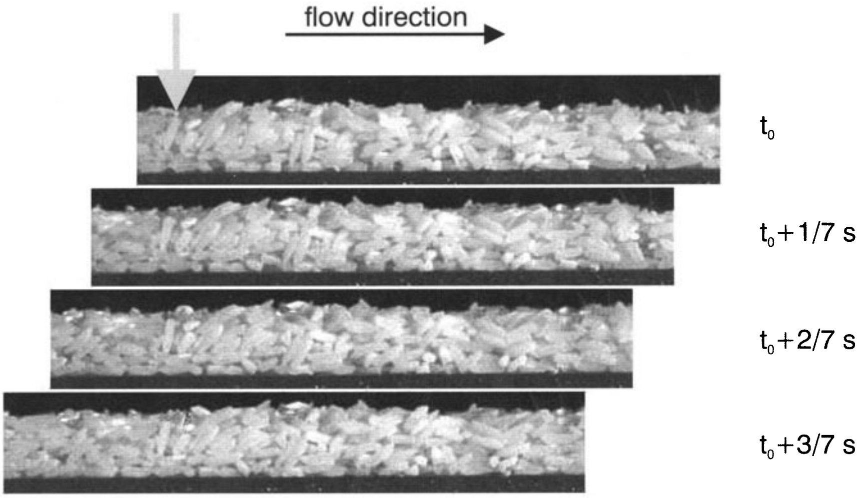

Fig. 2. Plug flow of rice. The whole body glides along the incline without any structural changes in the interior (see, e.g.,the vicinity of the grain marked by the gray arrow). The photographs are vertically aligned such that the same grains occur in columns

velocity of the flow (compare Fig. 3). Now, the velocities increase from the base to the free surface and the grains tend to orient in the shear flow. Although the examples shown in Figs. 2 and 3 pertain to rather shallow flows, the general phenomena can clearly be seen. In a shear layer the internal order is increased and the main orientation of the grains is determined by the flow direction (among other variables, as we shall see), whereas in a plug flow the uniform velocity field has no ordering capacity.

If we want to gain a better understanding of the flow induced order we have to introduce order parameters and we have to develop a constitutive theory which involves these order parameters as internal variables.

2.1 Definition of Order Parameters

Since a flowing anisotropic granular material can be regarded as a general anisotropic fluid we can follow classical ideas developed for molecular gases and liquid crystals to define suitable order parameters. Since our particles are (mostly) gliding we can neglect one rotational degree of freedom, i.e., the orientation of a

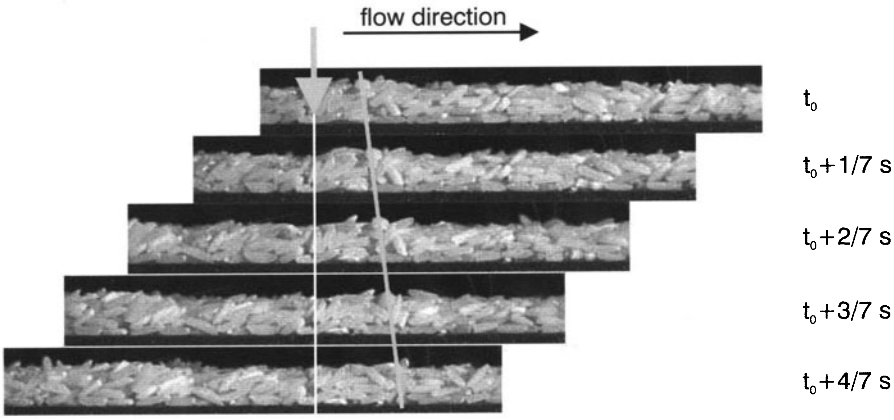

Fig. 3. Shear flow of rice. The photographs are vertically aligned with respect to grains at the base (white line). The top layer moves with a faster velocity, thus producing a simple shear (tilted gray line)

single grain is sufficiently prescribed by *one* unit vector which can be aligned along a characteristic axis of the grain (e.g. its symmetry axis). We adopt the notations of WALDMANN & HESS [12] and Hess [13,14] and start with an *orientation distribution function* (ODF) for the granular axes $\boldsymbol{n}$,

$$f : \; \mathbb{R}^3 \times \mathrm{S}^2 \times \mathbb{R} \longrightarrow \mathbb{R}_0^+ \,, \tag{50}$$

which is normalized

$$\oint_{\mathrm{S}^2} f(\boldsymbol{x}, \boldsymbol{n}, t)\, d^2 n = 1 \tag{51}$$

and symmetric

$$f(\boldsymbol{x}, \boldsymbol{n}, t) = f(\boldsymbol{x}, -\boldsymbol{n}, t)\,, \tag{52}$$

since for the grains we are considering here, orientations $\boldsymbol{n}$ and $-\boldsymbol{n}$ are indistinguishable. Then $f(\boldsymbol{x}, \boldsymbol{n}, t)\, d^2 n\, d^3 x$ denotes the probability to find grains with orientations in the solid angle $d^2 n$ inside the volume element $d^3 x$. Hence-force, we shall denote the *ensemble average* with respect to the ODF by angular brackets

$$< G > := \oint_{\mathrm{S}^2} f(\boldsymbol{x}, \boldsymbol{n}, t) G(\boldsymbol{x}, \boldsymbol{n}, t)\, d^2 n\,. \tag{53}$$

Since f itself is a rather complicated object we take some of its moments to characterize the local order in the material. For doing so, we choose a set of tensor functions and write the orientation distribution function as an infinite tensor series with respect to this basis. Our base functions are the Cartesian components of symmetric irreducible tensors, restricted to the unit sphere (for more information about this tensor family see the small booklet of HESS & KÖHLER [17] or

EHRENTRAUT & MUSCHIK [9]), which are closely related to spherical harmonics and form a $L^2(\mathrm{S}^2,\mathbb{R})$-basis for the square-integrable functions on the unit sphere. Here, the short comment shall be sufficient that symmetric irreducible tensors can be obtained from the ℓ-fold tensorial products of the unit vector $\boldsymbol{n}$ after removing all sorts of internal contractions such that the resulting tensor vanishes when a summation over an arbitrary index pair is performed. For second order tensors, the symmetric irreducible part of the tensor is identical to the symmetric traceless part! The crucial proposition for functions on the sphere reads now:

Let f be a square-integrable function on S^2. Then f can be expressed as a series of symmetric irreducible tensors (indicated by the bracket $\overline{\cdots}$)

$$f(\boldsymbol{n}) = \frac{1}{4\pi}\left\{f_0 + \sum_{\ell=1}^{\infty}\frac{(2\ell+1)!!}{\ell!}a_{\mu_1\cdots\mu_\ell}\ \overline{n_{\mu_1}\cdots n_{\mu_\ell}}\right\} \tag{54}$$

with Greek indices denoting Cartesian components, EINSTEIN*s summation convention used for them,*

$$a_{\mu_1\cdots\mu_\ell} = \oint_{S^2} f(\boldsymbol{n})\ \overline{n_{\mu_1}\cdots n_{\mu_\ell}}\ d^2n \quad (\ell\in\mathbb{N})\,, \tag{55}$$

$$f_0 = \oint_{S^2} f(\boldsymbol{n})\, d^2n\,, \tag{56}$$

and $(2\ell+1)!!$ denoting the product of all odd integers smaller or equal to $2\ell+1$.

For the ODF the absolute term fulfills $f_0 = 1$ due to normalization and all odd moments vanish due to symmetry. Thus we have

$$f(\cdot) = \frac{1}{4\pi}\left\{1 + \sum_{\ell\ \mathrm{even}}^{\infty}\frac{(2\ell+1)!!}{\ell!}a(\boldsymbol{x},t)_{\mu_1\cdots\mu_\ell}\ \overline{n_{\mu_1}\cdots n_{\mu_\ell}}\right\} \tag{57}$$

with the *alignment tensors*

$$a_{\mu_1\cdots\mu_\ell} = \oint_{\mathrm{S}^2} f(\boldsymbol{n})\ \overline{n_{\mu_1}\cdots n_{\mu_\ell}}\ d^2n \quad (\ell\in 2\mathbb{N})\,. \tag{58}$$

Of special interest is the first non-vanishing anisotropy moment, the alignment tensor of second order $\underline{\underline{\mathbf{a}}}$, the fourth alignment tensor influences the constitutive functions in special cases, but higher order alignment tensors are usually considered to be of minor importance.

2.2 Transversal Isotropy

The alignment tensor of ℓ-th order has in general $2\ell+1$ independent components. In many situations, however, the orientation distribution function possesses a transversally isotropic (uniaxial) symmetry which must not be confused with a symmetry of the particles. This symmetry can be expressed by the presence of of a spatial direction, specified by a unit vector $\boldsymbol{d}$, such that the dependence of f on $\boldsymbol{n}$ reduces to a dependence on the projection of $\boldsymbol{n}$ on $\boldsymbol{d}$:

$$f(\boldsymbol{x}, \boldsymbol{n}, t) = g(\boldsymbol{x}, \boldsymbol{n} \cdot \boldsymbol{d}, t) \text{ with a suitable function } g. \tag{59}$$

In this case the alignment tensors take a very simple form. Indeed, they are determined by the symmetry axis $\boldsymbol{d}$, called *director*, and *one* scalar parameter which is the ensemble average of the ℓ-th Legendre polynomial P_ℓ, i.e.

$$a_{\mu_1 \cdots \mu_\ell} = < P_\ell(\boldsymbol{n} \cdot \boldsymbol{d}) > \overline{d_{\mu_1} \cdots d_{\mu_\ell}} \ . \tag{60}$$

Traditionally, the second order parameter $< P_2 > \equiv S$ is called MAIER–SAUPE order parameter; if more than one scalar order parameter is used, they are denoted as $S_\ell := < P_\ell >$, i.e. S and S_2 refer to the same quantity.

To close this small investigation on order parameters we remark that S can vary in the interval $[-0.5, 1]$, that perfect alignment (the ODF collapses to the Dirac δ-function) forces all order parameters to be one ($S_\ell = 1$), and that a random distribution ensures $S_2 = S_4 = \cdots = S_\ell = \cdots = 0$.

2.3 A Remark on Evolution Equations for Alignment Tensors

The balance equations contain no information about the degree of order in the medium, but the macroscopic order parameters (alignment tensors) can be defined and therefore evolution equations are needed. To obtain these equations one can start from a mesoscopic level where the orientation variable $\boldsymbol{n}$ is treated at the same footing as the spatial variable $\boldsymbol{x}$. All physical quantities are then considered to be fields depending on time, position and orientation [2]. The newly formulated, mesoscopic balance equations contain additional flux terms due to orientation changes and can be found in different places in the literature [2–4,6,20]. For the mesoscopic mass density $\rho^{\text{meso}}(\boldsymbol{x}, \boldsymbol{n}, t) := \rho f$, conservation of mass results in

$$\frac{\partial \rho^{\text{meso}}}{\partial t} + \nabla_x \cdot \left(\boldsymbol{v}\rho^{\text{meso}}\right) + \nabla_n \cdot \left(\boldsymbol{\omega} \times \boldsymbol{n}\rho^{\text{meso}}\right) = 0\,, \tag{61}$$

which can be easily reformulated to yield an evolution equation for the ODF

$$\frac{\partial}{\partial t} f + \nabla_x \cdot (\boldsymbol{v} f) + \nabla_n \cdot (\boldsymbol{\omega} \times \boldsymbol{n} f) + f\left(\frac{\partial}{\partial t} + \boldsymbol{v} \cdot \nabla_x\right) \ln \rho = 0\,. \tag{62}$$

Since the alignment tensors are moments of f, the wanted equations can be derived by obtaining the moments of (62). However, this proves to be a rather complicated task and we shall not perform the calculations here, but discuss some of the problems which will arise.

Calculating the moments of f means multiplication by $\overline{n_{\mu_1} \cdots n_{\mu_\ell}}$ and integration over the unit sphere. This is no problem for the first term containing the time derivative and also the second term provides no difficulties if we assume that the velocity fields $\boldsymbol{v}$ does not depend on $\boldsymbol{n}$, which can be experimentally justified for many interesting cases. However, we cannot assume the same for $\boldsymbol{\omega} \times \boldsymbol{n}$. Since a uniform tangential vector field on the sphere can only be the null vector field (the fact that any continuous tangential vector field on the sphere S^2 vanishes at least at one point is a well-known theorem of differential geometry and it is often referred to as the proposition of the "combed hedgehog"). Consequently, we have to deal with nonlinear terms and this leads to non-linear coupling of *all* evolution equations for the alignment tensors. Thus closure relations are needed to obtain a finite set of equations, but even then one has to tackle a system on nonlinear, coupled, partial differential equations. Since we do not need these relations here, this particular line of thought will not be followed here any longer. The interested reader can find a general form of the alignment tensor balances in Blenk et al. [2] and informations on how to close the system of equations and to extract physical properties in different papers by Hess [13–16].

2.4 Viscosity Coefficients

We already saw that constitutive modeling for anisotropic granular flows can greatly benefit from liquid crystal theories [7]. Since the rheological behavior of a liquid crystal is, in addition to its optical properties, responsible for its performance in a liquid crystal display, many experiments have been performed to measure the viscosity coefficients and to examine the complex interaction between flow and local order in the fluid.

Normally, shear rates in liquid crystalline flows are low and the fluid behaves Newtonian. However, the internal structure of the fluid increases the number of viscosity coefficients compared to an isotropic liquid. One of the first attempts to study the rheology of nematics is due to Leslie [18]. He used a state space based on the equilibrium fields ρ and T (temperature), together with the simplest non-equilibrium variable for flows, the shear rate tensor $\underline{\underline{\gamma}} \; \overline{\nabla_x \boldsymbol{v}}$, and as structural variables, director $\boldsymbol{d}$ and its co-rotational ("Jaumann") derivative $\boldsymbol{D} := \dot{\boldsymbol{d}} - \boldsymbol{\Omega} \times \boldsymbol{d}$, where $\boldsymbol{\Omega}$ is the vorticity of the flow field. If we want a *linear* relation between spatial derivatives of the velocity field (note that $\boldsymbol{D}$ contains $\boldsymbol{\Omega} = \frac{1}{2}\nabla_x \times \boldsymbol{v}$!) and the non-equilibrium part of the stress tensor, the most general ansatz based on this state space is [5]

$$\begin{aligned} t_{\nu\mu}^{\text{non-eq.}} &= \alpha_1 d_\nu d_\mu d_\lambda d_\kappa \gamma_{\lambda\kappa} + \alpha_2 d_\nu D_\mu + \alpha_3 d_\mu D_\nu \\ &\quad + \alpha_4 \gamma_{\nu\mu} + \alpha_5 d_\nu d_\lambda \gamma_{\lambda\mu} + \alpha_6 d_\mu d_\lambda \gamma_{\lambda\nu} \\ &\quad + \zeta_1 d_\lambda d_\kappa \gamma_{\lambda\kappa} \delta_{\mu\nu} + \zeta_2 d_\nu d_\mu \nabla_\lambda v_\lambda + \zeta_3 \nabla_\lambda v_\lambda \delta_{\mu\nu} \,. \end{aligned} \tag{63}$$

The first six coefficients (α's) are called Leslie coefficients, the last two do not appear when incompressibility of the fluid is assumed. If we decompose (63) into the symmetric traceless, skew-symmetric and isotropic parts, we derive new coefficients, which are simple linear combinations of the old ones, but which are more adapted to the physical meaning of the terms, namely

$$\begin{aligned} \overline{t_{\nu\mu}^{\text{non-eq.}}} &= 2\eta\gamma_{\nu\mu} + 2\tilde{\eta}_1 \, \overline{d_\nu d_\lambda \gamma_{\lambda\mu}} + 2\tilde{\eta}_2 \, \overline{d_\nu D_\mu} \\ &\quad + \tilde{\eta}_3 \, \overline{d_\nu d_\mu d_\lambda d_\kappa \gamma_{\lambda\kappa}} + \zeta_2 \, \overline{d_\nu d_\mu} \, \nabla_\lambda v_\lambda \end{aligned} \tag{64}$$

$$(t_{\nu\mu}^{\text{non-eq.}})^a = -\gamma_1 (d_\nu D_\mu)^a - \gamma_2 \left(\overline{d_\nu d_\lambda} \, \gamma_{\lambda\mu} \right)^a \quad , \tag{65}$$

$$\frac{1}{3} t_{\lambda\lambda}^{\text{non-eq.}} = \eta_V \nabla_\lambda v_\lambda + \kappa d_\lambda d_\kappa \gamma_{\lambda\kappa} \,, \tag{66}$$

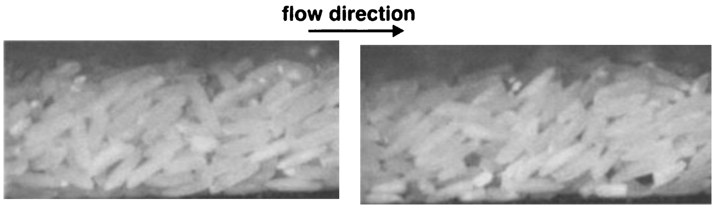

Fig. 4. Bottom layer of flowing rice. The grains are aligned and tilted along the flow direction

with

$$\eta = \frac{1}{2}\left(\alpha_4 + \frac{1}{3}(\alpha_5 + \alpha_6)\right) , \tag{67}$$

$$\tilde{\eta}_1 = \frac{1}{2}(\alpha_5 + \alpha_6) , \quad \tilde{\eta}_2 = \frac{1}{2}(\alpha_2 + \alpha_3) , \quad \tilde{\eta}_3 = \frac{1}{2}\alpha_1 , \tag{68}$$

$$\gamma_1 = \alpha_3 - \alpha_2 , \quad \gamma_2 = \alpha_6 - \alpha_5 , \tag{69}$$

$$\eta_V = \frac{1}{3}\zeta_2 + \zeta_3 , \quad \kappa = \zeta_1 + \frac{1}{3}(\alpha_1 + \alpha_5 + \alpha_6) . \tag{70}$$

Disappointingly enough, (64)–(66) are not very helpful if we want to study the influence of the order parameters on the viscosities. Since these equations are macroscopic relations the (scalar) order parameters must be buried in the coefficients and the functional dependence is unclear. However, if we take (64)–(66) as *mesoscopic* equations and replace the director field $\boldsymbol{d}$ by the variable $\boldsymbol{n}$ and $\boldsymbol{D}$ by $\boldsymbol{N}(\cdot) := (\boldsymbol{\omega} - \boldsymbol{\Omega}) \times \boldsymbol{n}$,

$$\begin{aligned} \overline{t^{\text{non-eq.}}_{\nu\mu}} &= 2\eta\gamma_{\nu\mu} 2\tilde{\eta}_1 \overline{n_\nu n_\lambda \gamma_{\lambda\mu}}\; 2\tilde{\eta}_2 \overline{n_\nu N_\mu} \\ &\quad + \tilde{\eta}_3 \overline{n_\nu n_\mu n_\lambda n_\kappa \gamma_{\lambda\kappa}} + \zeta_2 \overline{n_\nu n_\mu}\, \nabla_\lambda v_\lambda , \end{aligned} \tag{71}$$

$$(t^{\text{non-eq.}}_{\nu\mu})^a = -\gamma_1 (n_\nu N_\mu)^a - \gamma_2 \left(\overline{n_\nu n_\lambda}\, \gamma_{\lambda\mu}\right)^a , \tag{72}$$

$$\frac{1}{3} t^{\text{non-eq.}}_{\lambda\lambda} = \eta_V \nabla_\lambda v_\lambda + \kappa n_\lambda n_\kappa \gamma_{\lambda\kappa} , \tag{73}$$

we can calculate the macroscopic stresses as ensemble averages [8] if we assume that velocity fluctuations are negligible. For dense granular flows this approximation is experimentally well justified, and we can proceed further.

2.5 Flow Alignment

In order to examine flow alignment experimentally, rice was sent down an incline and the shear layer at the bottom was observed. Figure 4 shows two pictures taken in consecutive experiments. One sees clearly that the single grains are neither oriented randomly – the close confinement of the grains enforces their mutual alignment – nor that the alignment of the grains is independent on the flow. Since the friction between chute (made of plexiglass with a thin coating to prevent electrostatic attraction) and grains was rather low the shear rate is also not very high and a NEWTONian relation between shear rate and stress should apply. In addition, the geometry of the grains effectively hinders a rolling motion – the rice grains glide along the incline and the angular velocity $\boldsymbol{\omega}$ can be neglected. This experimental result confirms the assumptions of the extended SAVAGE–HUTTER theory we discussed in Sect. 1.2

Let us assume for simplicity that the orientation distribution of the grains is transversally isotropic. If only limited information about the functional form of the ODF is available, this assumption can always be justified by a maximum entropy argument as the most likely form agreeing with the data [6]. Figure 5 shows the histogram of orientations of the grains together with an transversally isotropic ODF fitted to the data.

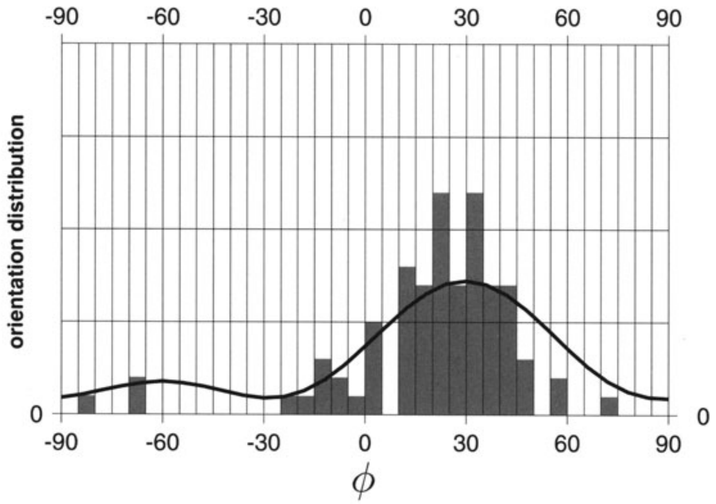

Fig. 5. Orientation distribution of rice grains in the shear zone. The histogram is obtained from the pictures in Fig. 4, the curve represents the ODF up to alignment tensors of fourth order which were obtained from the histogram

Then we can use scalar order parameters and a director $\boldsymbol{d}$ to express the alignment tensors, and we make the ansatz for $\boldsymbol{d}$

$$\boldsymbol{d} = \cos\phi\, \boldsymbol{t} + \sin\phi\, \boldsymbol{n} \tag{74}$$

with a flow alignment angle ϕ and x- and z-coordinate measured in flow (downhill) and gradient direction (perpendicular to the chute), respectively. It can be shown that another equilibrium solution of the symmetry relation (75) exists, where $\boldsymbol{d}$ points along the third, horizontal direction, but this equilibrium is unstable.

We already argued that in granular flows individual rotations of the grains are greatly constrained and that the contribution of the spin balance results in a simple symmetry statement for the stresses. Since the constitutive equations (71) – (73) do not obey this symmetry restriction by construction, we can extract additional information from the averaged relation

$$< (t_{\nu\mu}^{\text{non-eq.}})^a >= -\gamma_1 < n_\nu N_\mu >^a - \gamma_2 < \overline{n_\nu n_\lambda}\ \gamma_{\lambda\mu} >^a \ . \tag{75}$$

We can perform the calculations to evaluate the averaged expression for the stress tensor and insert the special ansatz (74) for the director to obtain equations which still contain the viscosity coefficients of an ordered reference fluid. Now, BAALSS & HESS [1] related these "ordered" coefficients to a reference viscosity η_{ref} and the axes ratio Q of ellipsoids resembling the shape of a single particle

$$\eta^{\mathrm{ord}} = \left(1 + \frac{1}{6}\left(Q - Q^{-1}\right)^2\right)\eta^{\mathrm{ref}} , \tag{76}$$

$$\tilde{\eta}_1^{\mathrm{ord}} = \frac{1}{2}\left(Q - Q^{-1}\right)^2 \eta^{\mathrm{ref}} , \tag{77}$$

$$\tilde{\eta}_2^{\mathrm{ord}} = \frac{1}{2}\left(Q^{-2} - Q^2\right)\eta^{\mathrm{ref}} , \tag{78}$$

$$\tilde{\eta}_3^{\mathrm{ord}} = -\tilde{\eta}_1^{\mathrm{ord}} , \tag{79}$$

$$\gamma_1^{\mathrm{ord}} = \left(Q - Q^{-1}\right)^2 \eta^{\mathrm{ref}} = 2\tilde{\eta}_1^{\mathrm{ord}} , \tag{80}$$

$$\gamma_2^{\mathrm{ord}} = \left(Q^{-2} - Q^2\right)\eta^{\mathrm{ref}} = 2\tilde{\eta}_2^{\mathrm{ord}} . \tag{81}$$

Thus, the symmetry condition (75) results in an equation containing the wanted flow alignment angle, order parameters from the averaging procedure and the aspect ratio Q of the grains – the reference viscosity cancels from (75). Thus we can conclude that material properties of the grains like roughness, which would appear in the reference viscosity, do not affect the flow alignment as long as grains do not stick together or the linear approximation used for the stress tensor breaks down.

After a lengthy, but simple calculation we arrive at an expression for the alignment angle

$$\cos(2\phi) = -\frac{2 - 5S}{3S}\frac{Q - Q^{-1}}{Q + Q^{-1}} . \tag{82}$$

The aspect ratio Q of a rice grain is easily measured. For the variety used it was $Q \approx 3.5$. The order parameter S can be directly measured, too, since we know the distribution function from Fig. 5. But in principle the situation so far is unsatisfactory. What conditions determine the local order in the rice? Certainly, initial conditions are not responsible for the order observed, since the grain distribution at the very beginning of the experiment was nearly random. Thus, the order must be established by the flow.

2.6 Coupling of Flow and Order Parameters

What mechanism can be responsible for the ordering of the grains? Since the particles interact only by collisions, the answer is simple: Energetic considerations based on interaction potentials can be ruled out, and the remaining thermodynamic force is entropy, which appears here in terms of excluded volumes.

A flowing granular material is in non-equilibrium since friction is present and the system dissipates energy. As long as the friction coefficient between bottom and grains is not very high, most of the energy is dissipated internally during the inelastic grain-grain collisions. Consequently, high dissipation inhibits the flow and smaller dissipation allows for quicker motion of the particles. If the local order parameters influence the dissipation – and we shall see that they do – the lowest possible dissipation would result in the best motion of the granules and therefore determine the order parameters.

Thus we claim a *minimum dissipation principle* for granular flows: The internal dissipation of the granular medium has to be assumed minimum to specify the local order parameters.

A short look at the balance for internal energy (9d) shows that the dissipation is mainly due to the dissipation potential $\Psi := \underline{\underline{t}} : \nabla \boldsymbol{v}$ when we neglect couple stresses. Thus we have to calculate the dissipation potential Ψ which is rather simple since we already know the stresses and $\nabla \boldsymbol{v}$ can be approximated by the assumption of a simple shear flow. However, it should be noted, that Ψ contains order parameters, the aspect ratio of the particles, the flow alignment angle, which can be expressed by (82), *and* the reference viscosity of (76)–(81). Thus Ψ depends in a complicated way on the order parameters and, of course, on material properties which were of no importance for the calculation of the alignment angle! However, η_{ref} affects the absolute value of the dissipation, but *not* the minimum of Ψ plotted against the order parameter. Figure 6 depicts the functional dependence of the dissipation in

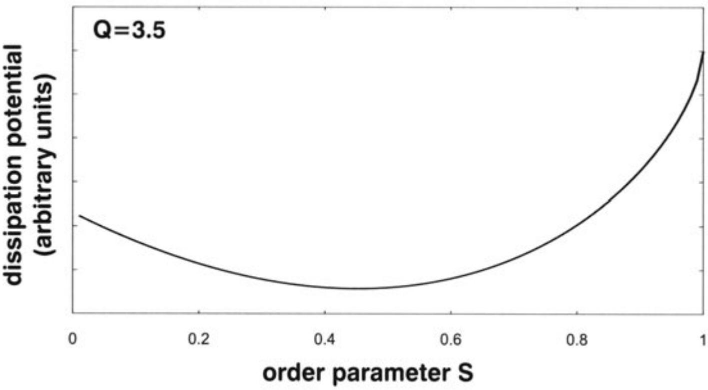

Fig. 6. Dissipation potential for axes ratio Q=3.5. The minimum is assumed for $S \approx 0.5$

the flow on the order parameter S. The minimum is assumed roughly for $S \approx 0.5$, the flow alignment angle which results is slightly less than 40°, which is in good agreement with the mean alignment angle of Fig. 5. Thus we have been able to solve the problem completely and the theoretical solution agrees nicely with the experimental observations.

3 Conclusions

Anisotropic fluids provide a wide field for investigations for anyone who is interested in continuum theories and structured media. On the previous pages a continuum thermo-mechanical framework was outlined which was inspired by the works of Ericksen, Leslie, Hess and many others on liquid crystals and has been adopted for granular materials. Certainly, it will have its applications also in other fields of material sciences where anisotropy is present.

It turned out that the SAVAGE–HUTTER theory applies as well to anisotropic granular media as to "normal" ones; the SAVAGE–HUTTER equations yield a suitable framework to calculate shallow granular flows in general. Nevertheless, the basic assumption of symmetric shear stresses cannot be upheld for anisotropic grains. Since, on the other hand, the spin balance reduces just to the same symmetry statement, the distinction between these two situations seems to be very artificial.

However, one should be careful not to confuse these two concepts: Any stress tensor which is a priori symmetric requires constitutive relations obeying this very symmetry *under all circumstances*! If we allow, however, for skew-symmetric parts in general and conclude, that these parts must vanish in certain situations, we can extract useful physical information like the flow alignment angle. In addition, one should keep im mind, that the symmetry statement is an approximation and that we have disregarded all couple stresses (tangential friction) to derive the statement. Hence, there are flow situations where neglection of the spin contributions leads to misjudgment. Simple examples are very thin flows when rolling of the particles becomes important.

For a simple but very important flow type (simple shear) we could determine the material response of the granular medium. The grains align within the flow field and the local order changes – resulting in a decreased effective viscosity of the yielding material. Since failure of granular structures often starts in shear bands, this phenomenon of "shear thinning" can significantly influence the dynamics of granular failure with induced anisotropy. Here, much future work will be needed to obtain a general model which can describe the transition from rest to fully developed flow.

Acknowledgments: Finally, we like to thank our colleagues for their support and many valuable discussions: Prof. K. HUTTER as the leader of the group "Fluid Dynamics", Dr. W. ECKART, Dr. J.M.N.T. GRAY, Dr. N. KIRCHNER, Dr. Y.-S. TAI, MSc. S. PUDASAINI and, of course, Dr. M. WEIS and Dipl.-Phys. B. MÜGGE, who kept our computers alive and kicking.

References

1. Baalss D.,Hess S. (1988) The viscosity coefficients of oriented nematic and nematic discotic liquid crystals; affine transformation model. Z Naturforsch 43a:662–670
2. Blenk S., Ehrentraut H., Muschik W. (1991) Statistical foundation of macroscopic balances for liquid crystals in alignment tensor formulation. Physica A 174:119–138
3. Blenk S., Ehrentraut H., Muschik W. (1992) Macroscopic constitutive equations for liquid crystals induced by their mesoscopic orientation distribution. Int J Engng Sci 30(9):1127–1143
4. Blenk S., Ehrentraut H., Muschik W. (1993) A continuum theory for liquid crystals describing different degrees of orientational order. Liquid Crystals 14(4):1221–1226
5. de Gennes, P.G. (1974) The Physics of Liquid Crystals. Clarendon Press, Oxford
6. Ehrentraut, H. 81996) A Unified Mesoscopic Continuum Theory of Uniaxial and Biaxial Liquid Crystals. Wissenschaft- und Technik Verlag, Berlin

7. Ehrentraut, H. (2001) Anisotropic Fluids: From Liquid Crystals to Granular Materials. In: Straughan B., Greve R., Ehrentraut H., Wang Y. (Eds.) Continuum Mechanics and Applications in Geophysics and the Environment, Springer, Berlin Heidelberg, 18 – 43
8. Ehrentraut H., Hess S. (1995) Viscosity coefficients of partially aligned nematic and nematic discotic liquid crystals. Phys Rev E 51(3):2203 – 2212
9. Ehrentraut H., Muschik W. (1998) On symmetric irreducible tensors in d-dimensions. ARI 51:149–159
10. Gray J.M.N.T., Wieland M., Hutter K. (1999) Gravity-driven free surface flow of granular avalanches over complex basal topography. Proc R Soc Lond A 455:1841–1874
11. Greve R., Koch T., Hutter K. (1994) Unconfined flow of granular avalanches along a partly curved surface. I. Theory. Proc R Soc Lond A 445:399–413
12. Hess S., Waldmann L. (1966) Kinetic theorie for a dilute gas of particles with spin. Z Naturforsch 21a:1529–1546
13. Hess S. (1975) Irreversible thermodynamics of nonequilibrium alignment phenomena in molecular liquids and in liquid crystals. Z Naturforsch 30a:728–733
14. Hess S. (1975) Irreversible thermodynamics of nonequilibrium alignment phenomena in molecular liquids and in liquid crystals II. Z Naturforsch 30a:1224–1232
15. Hess S. (1976) Fokker-Planck-equation approach to flow alignment in liquid crystals. Z Naturforsch 31a:1034–1037
16. Hess S. (1976) Pre- and post-transitional behaviour of the flow alignment and flow-induced phase transition in liquid crystals. Z Naturforsch 31a:1507–1513
17. Hess S., W. Köhler W. (1980) Formeln zur Tensor-Rechnung. Palm & Enke, Erlangen
18. Leslie F.M. (1968) Some constitutive equations for liquid crystals. Arch Rat Mech Anal 28:265–283
19. Muschik W., Ehrentraut H., Papenfuss C., Blenk S. (1995) Mesoscopic theory of liquid crystals. In: Brey J.J., Marro J., Rubi J.M., San Miguel M. (Eds.) 25 Years of Non-Equilibrium Statistical Mechanics, Lecture Notes in Physics 445, Springer, Berlin Heidelberg, 303–311
20. Muschik W., Ehrentraut H., Papenfuss C., Blenk S. (1996) Mesoscopic theory of liquid crystals. In: Shiner J.S. (Ed.) Entropy and Entropy Generation, Kluwer, Dordrecht, 101 – 109
21. Savage S.B., Hutter K. (1989) The motion of a finite mass of granular material down a rough incline. J Fluid Mech 199, 177–215
22. Tai Y.-C. (2000) Dynamics of Granular Avalanches and their Simulations with Shock-Capturing and Front-Tracking Numerical Schemes. Shaker Verlag, Aachen